ORIGINAL PAPER

H. Matsushima · T. Nohira · Y. Ito

Magnetic field effects on the crystal orientation and surface morphology of electrodeposited iron films

Abstract The effects of a magnetic field (5 T) on crystal orientation and surface morphology were investigated for iron films electrodeposited in ferrous aqueous solution. XRD measurements for the iron films showed that the preferred orientation parallel to the substrate was determined by the current density and not influenced by the magnetic field. By X-ray pole figure measurements, however, the crystal texture of the iron films electrodeposited at 10 mA cm^{-2} and 30 mA cm^{-2} was found to be controlled by the magnetic field. That is, the (110) planes were orientated in same direction of the magnetic field vector at angles of 30° and 35° to the direction normal to the substrate plane at 10 mA cm^{-2} and 30 mA cm^{-2}, respectively. When the morphology was observed by SEM, iron grains at 30 mA cm^{-2} changed from a triangular pyramid shape at 0 T to a complex star-like shape at 5 T.

Keywords Crystal orientation · Iron electrodeposition · Magnetic field · Surface morphology · Texture

Introduction

To pursue wider applications of electrodeposition, the authors consider that the superimposition of a magnetic field is very promising. A number of researchers have reported that some unique phenomena appeared when a magnetic field was superimposed on an electrodeposition process [1, 2, 3, 4, 5, 6, 7, 8, 9].

H. Matsushima · T. Nohira · Y. Ito (✉)
Department of Fundamental Energy Science,
Graduate School of Energy Science, Kyoto University,
Sakyo-ku, 606-8501 Kyoto, Japan
E-mail: y-ito@energy.kyoto-u.ac.jp

In our previous study, it was newly found that the crystal texture of an iron film electrodeposited at 10 mA cm^{-2} was controlled by a magnetic field (0.5–5 T) [10]. That is, the (110) plane was oriented in the same direction as the magnetic field vector at an angle of about 30° to the direction normal to the substrate plane. This result could not be explained by magnetocrystalline anisotropy since the axis of easy magnetization is (100) for iron. In addition, the result was inconsistent with the previous report of Li and Szpunar [11, 12], in which the (100) plane oriented in the same direction of the magnetic field vector.
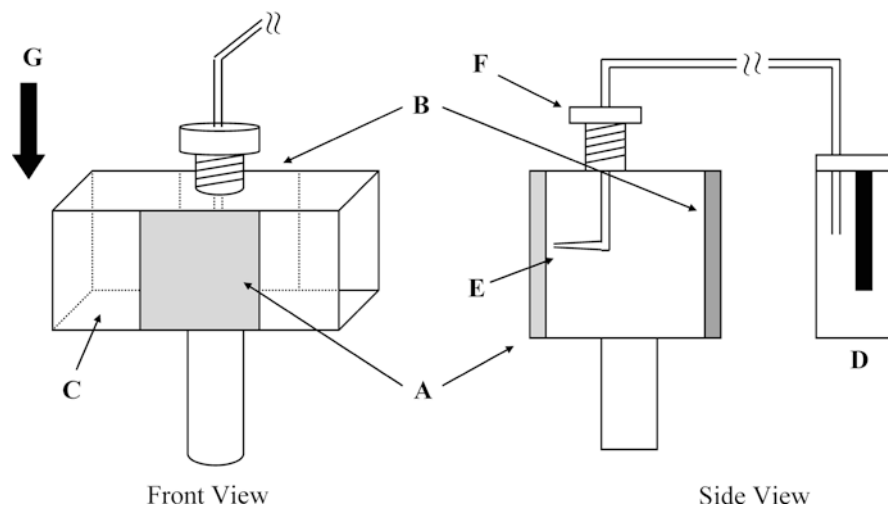
Based on the previous results, the effects of a magnetic field on iron electrodeposition were further investigated over a wider range of current density (3–100 mA cm^{-2}) in the present study. The relations between the effective current density of iron electrodeposition and the crystal orientation, as well as the surface morphology of the iron deposits, were newly investigated.

Experimental

Electrochemical experiments were carried out with a three-electrode system as illustrated in Fig. 1. The electrode assembly was composed of a short rectangular channel (10×10×30 mm^3, polystyrene) with two open ends and the assembly was immersed in a 300 mL electrolytic bath. The cathode was a sheet of copper (10×10×0.2 mm^3, 99.99% Cu, Nilaco). The anode was a sheet of pure iron (10×10×0.2 mm^3, 99.99% Fe, Nilaco). The reference electrode was Ag/AgCl with a saturated KCl aqueous solution. The electrolyte composition was 0.90 mol L^{-1} FeSO$_4$•7H$_2$O, 0.15 mol L^{-1} FeCl$_2$•4H$_2$O and 0.43 mol L^{-1} NH$_4$Cl. The pH of the electrolyte was adjusted to 1.5 with H$_2$SO$_4$. The solution temperature was maintained at 298 K. Iron film samples were prepared by galvanostatic electrolysis at various current densities (3–100 mA cm^{-2}) until the amount of electrical charge reached 150 C cm^{-2}. Electrodepositions were conducted in a static and uniform magnetic field parallel to the electrode surface with a magnitude of 5 T. The magnetic field was generated by a helium-free resistive magnet (CSM-6T, Sumitomo Heavy Industries) at the High Field Laboratory for Superconducting Materials, Institute for Materials Research, Tohoku University.

The preferred orientation of the electrodeposited iron film was measured by XRD using the Cu-Kα line (Multiflex, Rigaku, 40 kV,

Front View   Side View

40 mA; X'Pert, Philips, 50 kV, 40 mA). The morphology of the electrodeposited film was observed by SEM (S-2600H, Hitachi).

Results and discussion

Iron electrodeposition in the absence of a magnetic field

Iron electrodeposition was investigated in the absence of a magnetic field prior to the experiments in a magnetic field. In the first place, polarization curves were measured for total current density (i_T), iron electrodeposition current density (i_{Fe}) and hydrogen evolution current density (i_{H_2}), since the applied current is partially consumed by hydrogen gas evolution in the case of iron electrodeposition in acidic solution. Iron electrodepositions were conducted by potentiostatic electrolysis at −0.7 V to −1.35 V (vs. Ag/AgCl) until the amount of electrical charge reached 150 C cm^{-2}. A polarization curve for i_T, shown in Fig. 2, was obtained from the stationary current observed at the end of each electrolysis. Then, the iron current efficiency (η_{Fe}) was calculated from the weight of the iron deposits. The deviation from unity was considered to be due to hydrogen evolution ($\eta_{H_2} = 1 - \eta_{Fe}$). The values of i_{Fe} and i_{H_2} were calculated by $i_T \times \eta_{Fe}$ and $i_T \times \eta_{H_2}$, respectively, assuming a constant ratio of i_{Fe} to i_{H_2} during each electrolysis. As shown in Fig. 2, i_{Fe} values were lower than i_{H_2} from −0.7 V to −0.8 V. At values more negative than −0.9 V, i_{Fe} increased with i_T while i_{H_2} slightly increased to reach a limiting value of approximately 14 mA cm^{-2}. These results indicate that iron electrodeposition is mainly controlled by electric charge transfer, but that hydrogen evolution is controlled rather by mass transfer.

Secondly, in order to investigate the crystallographic orientation, iron film samples were electrodeposited at 3, 5, 10, 30, 50 and 100 mA cm^{-2} and were analyzed by XRD. Figure 3 shows three representative X-ray diffraction patterns of iron films electrodeposited at (a) 5, (b) 10 and (c) 30 mA cm^{-2}. It was found that the XRD
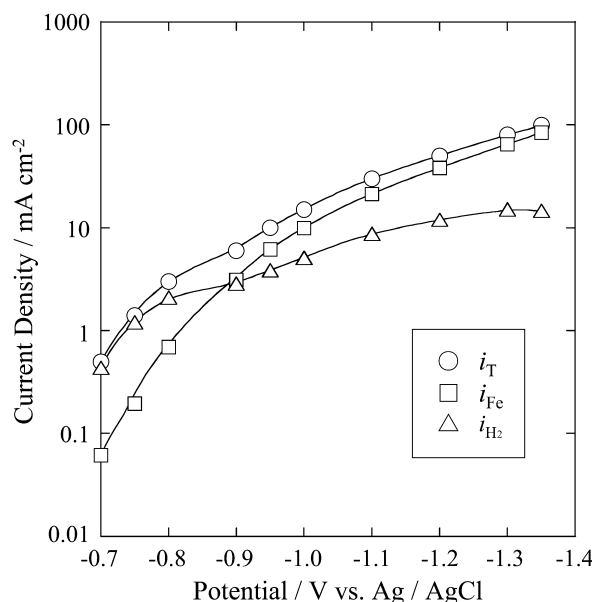

Fig. 2 Polarization curves for i_T, i_{Fe} and i_{H_2} in ferrous aqueous solution (pH 1.5, T = 298 K) in the absence of a magnetic field

patterns depended on the current density, that is, the strongest peaks in (a), (b) and (c) were the (110), (211) and (222) planes, respectively. In order to evaluate quantitatively the preferred orientation parallel to a substrate plane, the orientation index, *M*, was calculated as follows [13]:

$$M(hkl) = \frac{\frac{I(hkl)}{\sum I(h'k'l')}}{\frac{I_0(hkl)}{\sum I_{0(h'k'l')}}} \tag{1}$$

where $I(hkl)$ is the X-ray diffraction intensity from the experimental data, $I_0(hkl)$ is X-ray diffraction intensity from JCPDS cards, and $M(hkl)$ is the calculated orientation index. $\sum I(h'k'l')$ in the present case is the sum of the intensities of three independent peaks: (110), (211) and (222). Figure 4 shows the dependences of $M(110)$,
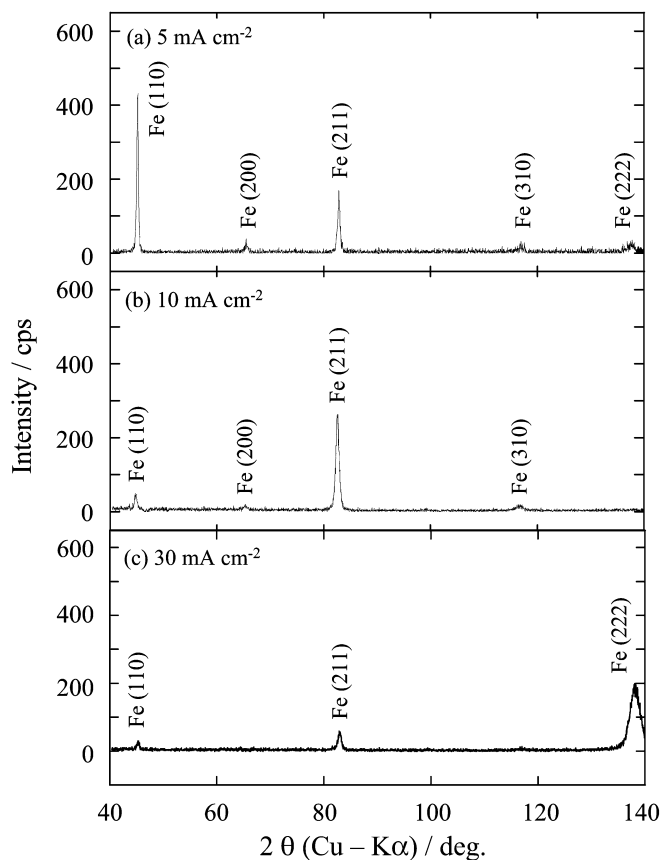
Fig. 3 X-ray diffraction patterns of electrodeposited iron films in the absence of a magnetic field: (**a**) 5 mA cm^{-2}, (**b**) 10 mA cm^{-2} and (**c**) 30 mA cm^{-2}
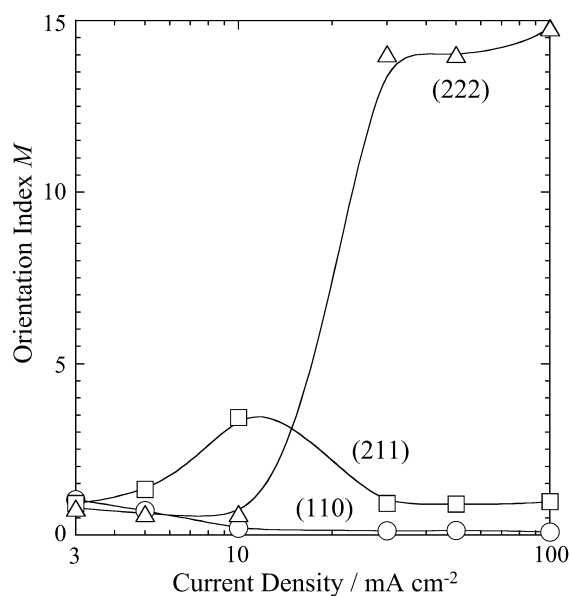

Fig. 4 Dependence of orientation index M on the current density for iron films electrodeposited in the absence of a magnetic field. *Circles*: (110) plane; *squares*: (211) plane; *triangles*: (222) plane

$M(211)$ and $M(222)$ on the current density. M was about unity for each crystal plane at 3 mA cm^{-2} and 5 mA cm^{-2}, which means random growth of the crystal
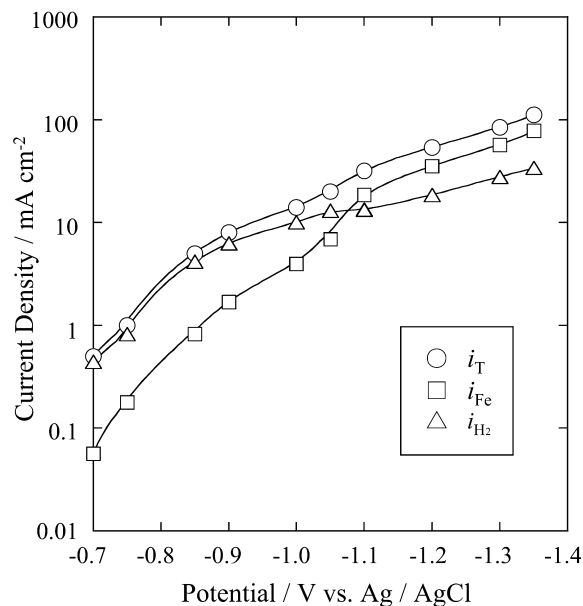

Fig. 5 Polarization curves for i_T, i_{Fe} and i_{H_2} in ferrous aqueous solution (pH 1.5, $T = 298$ °K) in a magnetic field of 5 T

planes. At 10 mA cm^{-2}, the (211) plane was the preferred orientation. At current densities higher than 30 mA cm^{-2}, the (222) plane was significantly oriented. Pangarov and Vitkova [14] reported that the electric overpotential for iron electrodeposition determines the axis of the preferred orientation, and that it is explained by the theory of two-dimensional nucleation. The dependence of M on the overpotential observed in this study agrees well with Pangarov and Vitkova's results.

Iron electrodeposition in the presence of a magnetic field

Similar experiments on iron electrodeposition were conducted in a magnetic field of 5 T. Figure 5 shows polarization curves for i_T, i_{Fe} and i_{H_2}. In the potential range of −0.7 V to −1.05 V, i_{Fe} was lower than i_{H_2}. Compared to the absence of a magnetic field (Fig. 2), i_{H_2} was larger at all potential regions. In addition, i_{H_2} did not show a limiting value, even at −1.35 V. The current efficiency of iron electrodeposition was 69% at −1.35 V, which is approximately 20% less than the efficiency in the absence of a magnetic field. The reduction of the iron current efficiency may be explained by magnetohydrodynamic (MHD) convection. That is, the MHD convection enhances mass transfer of H^+ ions, resulting in an increase of the hydrogen evolution current.

The iron film samples electrodeposited in a magnetic field were also analyzed by XRD. The orientation index, M, was calculated using Eq. 1. Figure 6 shows the dependence of M on the current density. No distinct difference was observed between the presence and absence of a magnetic field. This result is different from the reported result for nickel electrodeposition [5], in which
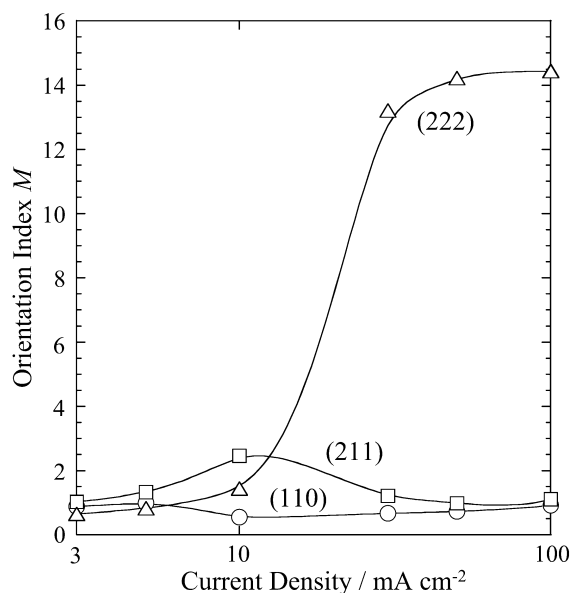
Fig. 6 Dependence of orientation index M on the current density for iron films electrodeposited in a magnetic field of 5 T. *Circles*: (110) plane; *squares*: (211) plane; *triangles*: (222) plane

the preferred orientation parallel to the substrate plane changed with the intensity of the magnetic field. In [5], the change of preferred orientation was explained by the difference of the pH change near the cathode surface due to the MHD convection which affects the hydrogen evolution. This explanation seems to be reasonable, since a solution of pH 4.5 was used and the pH value was likely to change significantly in [5]. On the other hand, a solution of pH 1.5 was used for the present iron electrodeposition, in which the pH change should be smaller than the above nickel case. Thus, it is explained that the preferred orientation parallel to the substrate is influenced by the electric effect (overpotential) and not by the small pH change induced by the magnetic field (MHD convection).

In order to investigate the crystal textures, X-ray pole figure measurements were conducted for the iron films electrodeposited at 10 mA cm^{-2} and 30 mA cm^{-2}. The pole figure can reveal crystal orientation not seen in a θ–2θ diffractometer. The figure is plotted in polar coordinates consisting of the tilt and rotation angles with respect to a given crystallographic orientation [15]. It should be noted that the thickness of the iron film obtained at 5 mA cm^{-2} was too thin to investigate the crystal texture due to a quite low current efficiency ($\sim$15%) of iron electrodeposition.

Figure 7 shows pole figures of the iron (110) plane electrodeposited at 10 mA cm^{-2} in (a) the absence of magnetic field and (b) a magnetic field of 5 T. The magnetic field was applied parallel to the substrate surface and its direction is indicated by an arrow in Fig. 7. In (a), there was a circle pattern at an angle of 30° to the direction normal to the substrate plane. The angle of 30° indicates that the (211) plane was oriented parallel to the substrate, which is consistent with the result in Fig. 6. This circle pattern shows that the (110) planes faced arbitrary directions randomly. On the other hand, in (b), there was an obvious crystal orientation in same direction as the magnetic field vector.

Figure 8 shows pole figures of the iron (110) plane electrodeposited at 30 mA cm^{-2}. In the absence of a magnetic field (Fig. 8a), there was a circular pattern at an angle of 35°. This angle means that the (222) plane was oriented parallel to the substrate, which is consistent with the result in Fig. 6. On the other hand, in a magnetic field of 5 T (Fig. 8b), there was a crystal orientation in same direction as the magnetic field vector. However, the circular pattern was more concentric and the crystal orientation did not appear clearly, compared with the result in Fig. 7. The unclear anisotropic pattern suggests that the crystal orientation of the (110) plane was influenced by the electric field in addition to the magnetic field at higher current density.

From the above results, it is found that the iron crystal orientation is controlled by a magnetic field at 10 mA cm^{-2} and 30 mA cm^{-2}. Although a definite explanation for the crystal orientation of the (110) plane cannot be given at present, the convection induced by MHD might be responsible for the orientations. The orientation of iron has been reported to be influenced by
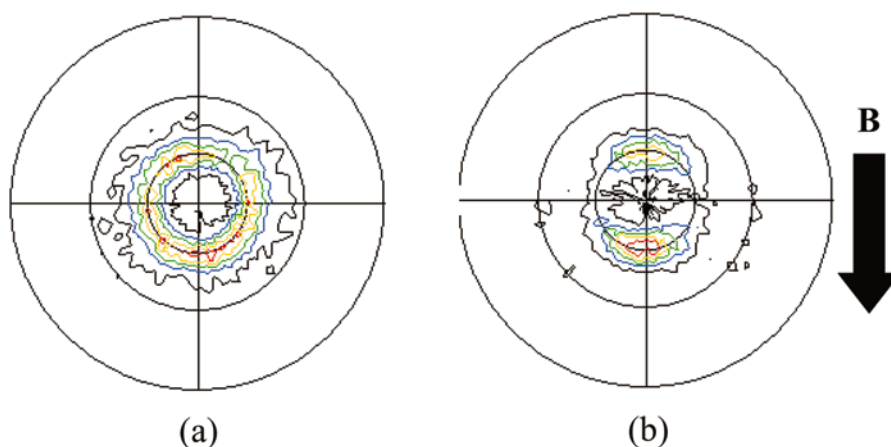
Fig. 7 Pole figures of iron (110) plane electrodeposited at 10 mA cm^{-2} (**a**) in the absence of a magnetic field and (**b**) in a magnetic field of 5 T. The *arrow* shows the magnetic field direction

(a)   (b)

Fig. 8 Pole figures of the iron (110) plane electrodeposited at 30 mA cm^{-2} (**a**) in the absence of a magnetic field and (**b**) in a magnetic field of 5 T. The *arrow* shows magnetic field direction
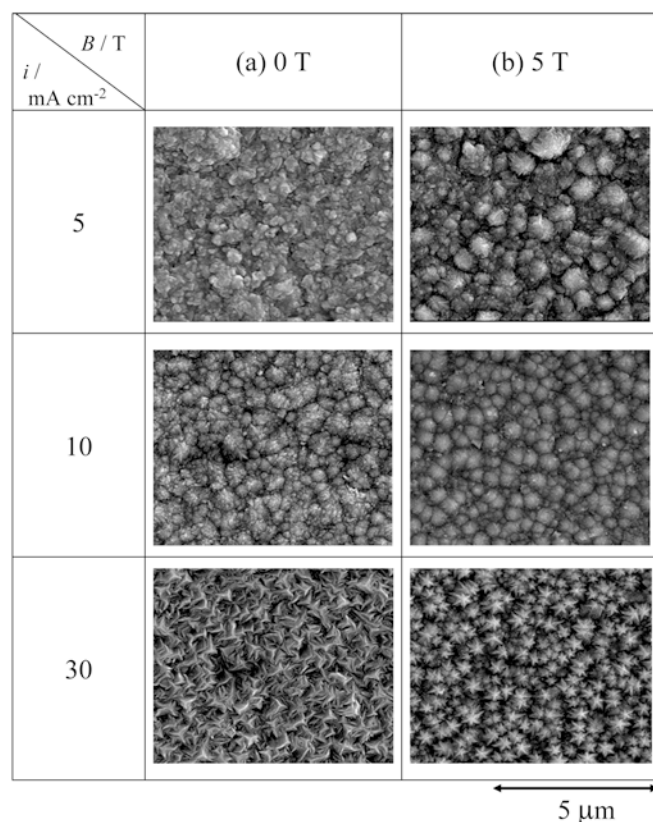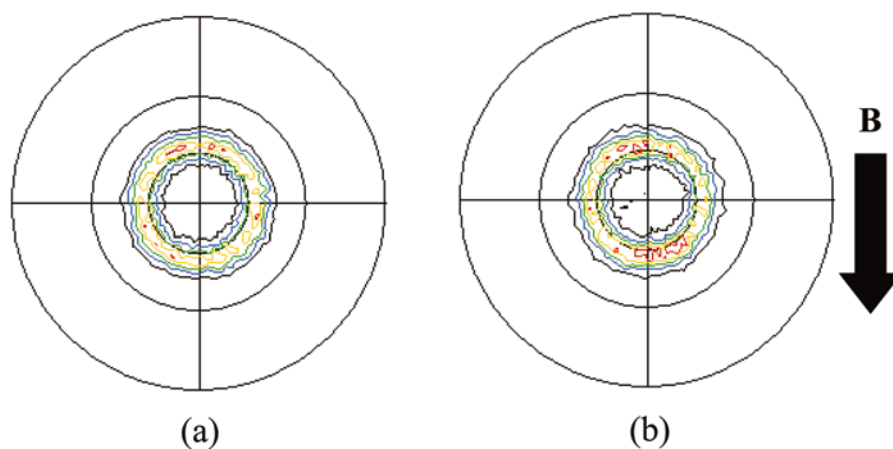

B

(a)   (b)

5 μm

Fig. 9 SEM images of iron films electrodeposited at 3, 10 and 30 mA cm^{-2} (**a**) in the absence of a magnetic field and (**b**) in a magnetic field of 5 T

specific adsorptions of hydroxides and atomic hydrogens [12, 13]. In the present case, it is considered that the hydroxides decrease and the atomic hydrogens increase on the lateral surfaces of iron facing the MHD convection, since the H$^+$ ion transportation is enhanced. Therefore, the crystal orientation might be influenced by a magnetic field.

In order to study the surface morphology, SEM observations were also conducted. Figure 9 shows SEM images of iron films electrodeposited at 5, 10 and 30 mA cm^{-2} in (a) the absence of a magnetic field and in (b) a magnetic field of 5 T. At 5 mA cm^{-2}, the surface morphology of iron grains did not seem to be affected by a magnetic field according to the present SEM images. However, at 10 mA cm^{-2}, the morphology of iron grains electrodeposited in the magnetic field appeared to be smoother. Such changes were more clearly shown by the atomic force microscopy (AFM) images reported in a separate paper [10]. At 30 mA cm^{-2}, the shape of the iron grains was significantly changed by the magnetic field. That is, in the absence of the magnetic field, the shape was a triangular pyramid that is characteristic of the (222) preferred orientation. On the other hand, in the magnetic field, the iron grains showed a complex star-like shape and the microscopic roughness was higher. The change of morphology might be related to the formation of hydrogen gas bubbles. According to Fig. 5, hydrogen evolution was enhanced in the magnetic field. It is considered that the gas bubbles clung to iron grains and inhibited free growth of the grains, resulting in the formation of complex morphology in the magnetic field.

Conclusions

Iron was electrodeposited in a magnetic field of 5 T in a ferrous aqueous solution (pH 1.5, T = 298 K). In the magnetic field, MHD convection enhanced hydrogen evolution that was controlled by mass transfer. The preferred orientations parallel to the substrate plane were the (211) plane at 10 mA cm^{-2} and the (222) plane at higher than 30 mA cm^{-2}, regardless of the magnetic field. By X-ray pole figure measurements, however, it was found that the crystal texture of the iron film electrodeposited at both 10 mA cm^{-2} and 30 mA cm^{-2} was controlled by the magnetic field. That is, the (110) planes were oriented in the same direction as the magnetic field vector at angles of about 30° and 35° to the direction normal to the substrate plane at 10 mA cm^{-2} and 30 mA cm^{-2}, respectively. The shape of the iron grains at 30 mA cm^{-2} was changed from a triangular pyramid in the absence of the magnetic field to a complex star-like shape in the magnetic field.

References

1. Fahidy TZ (2001) Prog Surf Sci 68:155
2. O'Reilly XX, Hinds G, Coey JMD (2001) J Electrochem Soc 148:C647
3. Kwou HW, Kim SK, Jeong Y (2000) J Appl Phys 87:6185
4. Bodea S, Vignon L, Ballou R, Molho P (1999) Phys Rev Lett 83:2612
5. Devos O, Olivier A, Chopart JP, Aaboubi O, Maurin G (1998) J Electrochem Soc 145:401
6. Mogi I, Kamiko M (1996) J Crystal Growth 166:276
7. Tacken RA, Janssen LJJ (1995) J Appl Electrochem 25:1
8. Aaboubi O, Chopart JP, Douglade J, Olivier A (1990) J Electrochem Soc 137:1796
9. Chiba A, Kitamura K, Ogawa T (1986) Surf Coat Technol 27:83
10. Matsushima H, Nohira T, Mogi I, Ito Y (2003) Surf Coat Technol (in press)
11. Li DY, Szpunar JA (1997) Electrochim Acta 42:37
12. Li DY, Szpunar JA (1997) Electrochim Acta 42:47
13. Yoshimura S, Yoshihara S, Shirakashi T, Sato E (1994) Electrochim Acta 39:589
14. Pangarov NA, Vitkova SD (1966) Electrochim Acta 11:1719
15. Bunge HJ, Esling C (1982) Quantitative texture analysis. Deutsche Gesellschaft fur Metallkunde, Frankfurt